Original Article

Evaluation of iodine-123-labeled metaiodobenzylguanidine single-photon emission computed tomography/computed tomography based on the International Society of Pediatric Oncology Europe Neuroblastoma score in children with neuroblastoma

Ziang Zhou, Guanyun Wang, Luodan Qian, Jun Liu, Xu Yang, Shuxin Zhang, Mingyu Zhang, Ying Kan, Wei Wang, Jigang Yang

Department of Nuclear Medicine, Beijing Friendship Hospital, Capital Medical University, Beijing, China

Contributions: (I) Conception and design Z Zhou, J Liu, M Zhang, J Yang; (II) Administrative support: Z Zhou, W Wang, S Zhang, L Qian; (III) Provision of study materials or patients: Z Zhou, X Yang, G Wang, Y Kan; (IV) Collection and assembly of data: Z Zhou; (V) Data analysis and interpretation: Z Zhou, X Yang, G Wang; (VI) Manuscript writing: All authors; (VII) Final approval of manuscript: All authors.

Correspondence to: Jigang Yang. Department of Nuclear Medicine, Beijing Friendship Hospital, Capital Medical University, 95 Yong'an Road, Xicheng District, Beijing 100050, China. Email: yangjigang@ccmu.edu.cn.

Background: This study sought to examine whether iodine-123-labeled metaiodobenzylguanidine (^{123}I-MIBG) single-photon emission computed tomography/computed tomography (SPECT/CT), which is based on the International Society of Pediatric Oncology Europe Neuroblastoma (SIOPEN) score, could improve the diagnostic efficiency of children with neuroblastoma (NB), and to compare the diagnostic ability of minimal residual disease (MRD) detection and ^{123}I-MIBG SPECT/CT.

Methods: We retrospectively analyzed 238 scans of patients who underwent ^{123}I-MIBG SPECT/CT at the Department of Nuclear Medicine, Beijing Friendship Hospital, from January 2021 to December 2021. The diagnostic study was not registered with a clinical trial platform, and the study protocol was not published. The standard was established based on pathology, other relevant imaging examinations, and follow-up. The SIOPEN scores were calculated separately based on planar and tomographic imaging.

Results: In a comparison to the standard mentioned in the method, the diagnostic accuracy of planar and tomographic imaging was 151 of 238 (63.5%) and 228 of 238 (95.8%), respectively, and the κ values of the SIOPEN score were 0.468 and 0.855 (P<0.001), respectively. The SIOPEN scores differed significantly among the various subgroups. The polymerase chain reaction (PCR) method used to detect the bone marrow *PHOX2B* gene was able to find bone/bone marrow metastases (P=0.024, κ=0.282), while the flow cytometry (FCM) assay method was not statistically significant (P=0.417, κ=0.065).

Conclusions: ^{123}I-MIBG SPECT/CT, which relies on the semiquantitative assessment of the SIOPEN score, is of clinical importance in the management of pediatric NB. MRD detection can be used to detect early metastasis and recurrence in the bone or bone marrow; however, ^{123}I-MIBG SPECT/CT has better diagnostic value. We intend to conduct further investigations on their prognostic value in the future.

Keywords: Metaiodobenzylguanidine (MIBG); single-photon emission computed tomography/computed tomography (SPECT/CT); neuroblastoma (NB); International Society of Pediatric Oncology Europe Neuroblastoma (SIOPEN); minimal residual disease (MRD)

Submitted Oct 14, 2022. Accepted for publication Apr 10, 2023. Published online May 08, 2023.
doi: 10.21037/qims-22-1120
View this article at: https://dx.doi.org/10.21037/qims-22-1120

Introduction

Neuroblastoma (NB), which originates from the sympathetic nervous system, is the most common extracranial solid malignant tumor in children and has an incidence rate of approximately 7% (1). The abdominal adrenal region (50%) is the most frequent site of NB (2). NB is highly malignant, and bone or bone marrow metastases are generally present at the time of diagnosis (2). NB is diagnosed on the basis of pathology, imaging characteristics, and laboratory tests. The management of children varies according to the staging and risk classification, but treatment typically includes chemotherapy, radiotherapy, immunotherapy, iodine-131-labeled metaiodobenzylguanidine (^{131}I-MIBG) therapy, and hematopoietic stem cell transplantation (3,4). Imaging plays an important role in the diagnosis, staging, and prognosis of patients with NB (5).

Conventional imaging, including ultrasonography, computed tomography (CT), and magnetic resonance imaging (MRI), can reveal the site of a tumor and its relationship to the surrounding tissues; however, it still has limitations in evaluating the staging of disease and the activity of the tumor cells or the residual foci as well as in administering targeted therapy. ^{123}I-MIBG single-photon emission computed tomography/computed tomography (SPECT/CT) is a type of functional imaging with high sensitivity and specificity in NB (6,7). The plane-based semiquantitative scoring system assesses tumor activity well, and thus it has important clinical significance in treatment-effect evaluations and prognosis assessments (8). However, ^{123}I-MIBG planar imaging has some limitations, including poor resolution and anatomical localization, especially for the diagnosis of suspicious lesions nearby physiological uptake. Currently, the clinical interpretation of images is mainly conducted with the Curie and the International Society of Pediatric Oncology Europe Neuroblastoma (SIOPEN) semiquantitative scoring, and international multicenter studies have suggested that the SIOPEN score and the modified Curie score are the two most commonly used systems and have good reproducibility and concordance among different observers (9).

Minimal residual disease (MRD) is a factor that causes relapse and bone or bone marrow metastasis in children with complete remission. Thus, the monitoring of MRD levels not only guides treatment but can also be used to evaluate new drugs and the cutting-edge designs of new treatment protocols (10). Studies have shown that MRD results can be used as an independent prognostic indicator after two rounds of immunotherapy (11), but only limited research on the specific clinical value of MRD has been conducted (12). Given the extreme heterogeneity of NB, many MRD tests have used different methods and samples in the last 20 years, but their clinical implications remain unclear (13). At present, there are 3 main ways to detect MRD (14); that is, immunocytochemistry, flow cytometry (FCM) assays, and quantitative real-time polymerase chain reaction (qRT-PCR). Previous study (15) have mainly used PCR to detect *PHOX2B* gene expression in the bone marrow and peripheral blood, while FCM assays have been used to detect tumor cells surface antigens, such as CD45/CD56/ganglioside 2 (GD2) and CD45/immunoglobin G (IgG). However, the abovementioned MRD measurement methods are not used widely and are not accurate in clinical practice, especially in solid tumors (16).

This study sought to examine whether ^{123}I-MIBG SPECT/CT, which is based on the SIOPEN score, improves the diagnostic ability in children with NB. We also evaluated the added clinical value of MRD detection, which is based on the standard of pathology, other relevant imaging examinations, and follow-up, and analyzed the efficiency of PCR and FCM in MRD detection. We present the following article in accordance with the STARD reporting checklist (available at https://qims.amegroups.com/article/view/10.21037/qims-22-1120/rc).

Methods

General information

We consecutively reviewed the data of children with stage 3 or stage 4 NB who had undergone ^{123}I-MIBG SPECT/CT at the Beijing Friendship Hospital of Capital Medical University from January 2021 to December 2021. A total of 238 scans of patients with NB were included in this study. The patients were aged from 6 months to 13 years and had a median age of 4 years. To be eligible for inclusion in this study, the patients had to meet the following inclusion criteria (17): (I) have postoperative pathological confirmation of NB; (II) have undergone ^{123}I-MIBG SPECT/CT at our department; and (III) not have undergone any treatment between the MRD and imaging, and MRD and MIBG examination should have an interval of <6 months (18). Patients were excluded from the study if they met any of the following exclusion criteria: (I) were unable to cooperate with the examination; (II) their guardians did not sign the informed consent; and/or

(III) they were ultimately lost to follow-up. The children who met the above requirements also underwent MRD examinations.

All the guardians of the patients were informed of the study and signed the informed consent form before the ^{123}I-MIBG SPECT/CT examination. The study was conducted in accordance with the Declaration of Helsinki (as revised in 2013). The study was approved by the Institutional Board of Beijing Friendship Hospital of Capital Medical University (No. 2022-P3-324-01), and the requirement of individual consent for this retrospective analysis was waived.

Imaging and testing methods

Thyroid blockade is essential to protecting the thyroid from unnecessary irradiation. Thus, all the children took Lugol's iodine solution in 3 divided doses with meals 2 days before and after imaging. The dose was determined in accordance with the European Association of Nuclear Medicine Pediatric Committee guidelines (18). The imaging agent, ^{123}I-MIBG 5.2 MBq/kg (37–370 MBq) (19-21), which was provided by Beijing Atomic High Technology Co., was injected intravenously on the day before the acquisition of the images based on each patient's age and weight. The SPECT/CT machine was a Siemens Symbia T16 (Siemens Healthcare, Germany) with a low-energy all-purpose collimator. The planar acquisition conditions were as follows: 256×1,024 matrix, 150 keV ±10% photopeak, and zoom 1.5–2. Tomography was performed instantly after the acquisition of the planar images. The SPECT had a circular orbit with a 360° arc, a 128×128 matrix, and a zoom of 1.6, with frames being acquired every 6 degrees for 20 seconds. CT scans were acquired for attenuation correction and localization purpose, and resolution restoration under the following parameters: 80 kV, 130 mAs. If the planar images were negative, the tomographic site was selected as the operative area, and if the planar images were positive, the tomographic site was chosen as the area of suspicious lesions. The following MRD method was used: PCR for the *PHOX2B* gene fragment in the bone marrow and peripheral blood samples (15); and FCM assays for the GD2, CD45, CD56, and surface-specific markers of NB (22,23).

Image interpretation

All the images were reviewed by two nuclear physicians in a double-blind manner according to the international SIOPEN scoring standard to determine the semiquantitative scores. When the scores were inconsistent, they were rereviewed by a third nuclear physician who had more experience until consistent results were obtained. The diagnostic criteria for the abnormal concentration of the contrast agent were as follows: the concentration was much greater than the background tissue or the corresponding part of the contralateral side, and the suspicious lesion was considered to be malignant after the exclusion of the physiological uptake by the liver, glands, or intestine. The following SIOPEN scoring method was used (24,25): the human skeleton was divided into 12 segments, and each region was rated from 0 to 6 according to the focal or diffuse lesions.

To be defined as a lesion, 1 or more of the following criteria had to be met: (I) a pathological histological diagnosis of the lesion area was obtained; (II) another relevant imaging diagnosis, including an ultrasound, radiology, 2-deoxy-2-[fluorine-18]fluoro-D-glucose positron emission tomography (PET)/CT, or follow-up ^{123}I-MIBG SPECT/CT diagnosis, was obtained; and/or (III) the 18-month clinical follow-up was clear for the lesion. The MRD results were used to evaluate the consistency of the results after the finalized metastasis site images in combination with the score of the MIBG tomography images were obtained as the final standard, and the sensitivity to detect bone metastases, negative or positive, was compared.

Statistical and data analysis

The statistical analysis was performed using SPSS 22.0 (IBM Corp., Armonk, NY, USA). The qualitative data are expressed as the number of cases and percentage [n (%)]. The chi-squared test was used to evaluate the associations between the categorical variables. The inter- and intra-observer values were estimated using the Cohen's kappa coefficient (26) [with 95% confidence intervals (CIs)]. A κ value <0.21 indicated a poor agreement, a κ value of 0.21–0.40 indicated a fair agreement, a κ value of 0.41–0.60 indicated a moderate agreement, a κ value of 0.61–0.80 indicated a substantial agreement, and a κ value of >0.80 indicated an excellent agreement. The area under the receiver operating characteristic curve was calculated to assess the predictive value of the MRD detection. We then calculated the sensitivity, specificity, positive predictive value (PPV), and negative predictive value (NPV). All the statistical tests were two-tailed, and a P value <0.05 indicated a significant difference. There were no missing

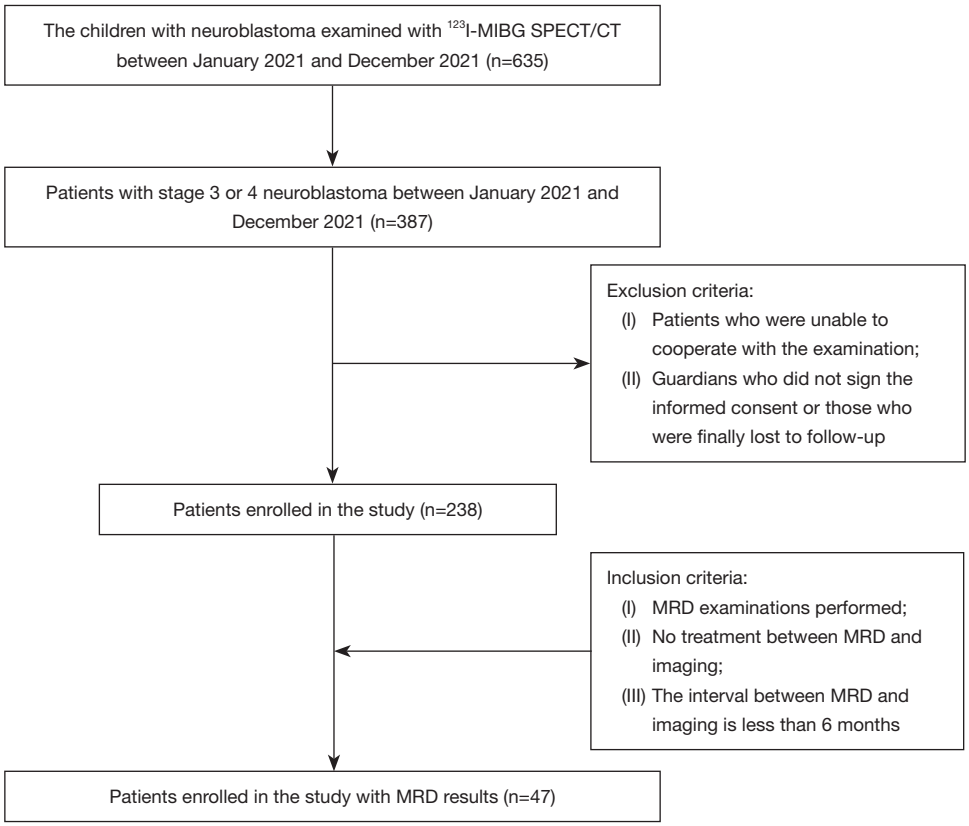

Figure 1 Flow diagram for the inclusion and exclusion of patients. ^{123}I-MIBG, iodine-123-labeled metaiodobenzylguanidine; SPECT, single-photon emission computed tomography; CT, computed tomography; MRD, minimal residual disease.

data or uncertain results (either positive or negative).

Results

Comparison of changes and the diagnostic efficacy of the SIOPEN score after planar and tomographic imaging

A total of 238 patients with stage III and IV NB were enrolled in our study (*Figure 1*), among whom 47 (19.7%) were in stage III, 171 (71.8%) were in stage IV, and 20 (8.4%) were in stage IV. Of the patients, 135 (56.7%) were male and 103 (43.3%) were female. The patients had a median age of 4 years. The patients' characteristics are summarized in *Table 1*.

The SIOPEN scores after the planar and tomographic imaging were calculated separately. The criteria defined as a lesion were used as a basis to explore the consistency of the planar and tomographic imaging. A paired comparison was conducted of 238 planar images and ^{123}I-MIBG SPECT/CT images, and the accuracy of the ^{123}I-MIBG planar imaging and ^{123}I-MIBG SPECT/CT was 151/238 (63.5%) and 228/238 (95.8%), respectively (*Table 2*). The tomography significantly improved the diagnostic accuracy to find bone/bone marrow metastases (95% CI, 0.17–0.25) (*Figure 2*). In total, 157 of the 238 (66.0%) patients had the same SIOPEN score after SPECT/CT, among whom 146 (61.3%) had a score of 0 for both the planar imaging and SPECT/CT. However, the SIOPEN score of 81 of the 238 (34.0%) patients changed after SPECT/CT, among whom, 20 (8.4%) had a decreased score and 61 (25.6%) had an increased score.

Comparison of the SIOPEN scores between the different groups for ^{123}I-MIBG planar imaging and SPECT/CT

According to the absolute value of the SIOPEN score, the children were divided into the 0-score, low-score (a score of 1–4), and high-score (a score of >4) subgroups. For the planar imaging, there were 170 (71.4%) scans in the 0-score group, 39 (16.4%) in the low-score group, and

29 (12.2%) in the high-score group. For the tomographic imaging, there were 158 (66.4%) scans in the 0-score group, 36 (15.1%) in the low-score group, and 44 (18.5%) in the high-score group. Notably, SPECT/CT changed the scores of 24 scans, which had a SIOPEN score of 0 in the planar imaging. Specifically, 16 scans had an increased score of ≤4 (the low-score group), and 8 scans had an increased score of ≥5 (the high-score group). The chi-squared test results revealed a significant difference between the different groups (P<0.001) (*Table 3*). As previously reported in international studies (9), the patients with a SIOPEN score of ≤4 have a better prognosis than SIOPEN scores of >5, and thus this category (SIOPEN score of ≤4) was divided into the following 6 subgroups: the 0, 1, 2, 3, 4 and ≥5 subgroups. The consistency of the SIOPEN score with the golden standard was compared across different imaging situations for the planar and tomographic images, respectively (*Tables 4,5*). The tomographic images (κ=0.855) showed better agreement with the standard method than did the planar images (κ=0.468). SPECT/CT had changed the choice of subsequent treatments for the different groups of children. To some extent, the SPECT/CT changed the prognosis by changing the intuitive value of the SIOPEN score.

Table 1 Patient characteristics

Characteristics	N=238
Gender	
Male	135 (56.7)
Female	103 (43.3)
Age	
Median (years)	4
<18 months	28 (11.8)
≥18 months	210 (88.2)
Primary focal site	
Adrenal	94 (39.5)
Nonadrenal	144 (60.5)
Preoperative bone aspiration results	
Negative	142 (59.7)
Positive	69 (29.0)
Unknown	27 (11.3)
Staging	
3	47 (19.7)
4	171 (71.8)
4s	20 (8.4)
Chemotherapy only	
Yes	104 (43.7)
No	134 (56.3)

Data are presented as the median or n (%) of participants.

The efficacy of PCR and FCM in MRD detection

In total, 47 examinations met the requirements in this study. Among the 44 examinations for which MRD tests were used to detect the *PHOX2B* gene in the bone marrow using the PCR method, 27 examination results were consistent with the final results obtained using the standard method, and 17 examination results were inconsistent, and the difference was statistically significant (P=0.024, κ=0.282). The sensitivity of diagnostic ability for bone metastases was 40%, the specificity was 89.5%, the accuracy rate was 62.2%, the PPV was 83.3%, and the NPV was 53.1% (*Table 6*). In relation to the MRD tests that used venous blood to detect the *PHOX2B* gene using the PCR method, 7 examinations were discarded. FCM assays were used to detect NB cells in 43 examinations, and 21 results were consistent with those obtained using the standard method, and 22 were inconsistent. Their agreement was verified separately using the chi-squared test (P=0.416, κ=0.065)

Table 2 The accuracy of ^{123}I-MIBG planar imaging and ^{123}I-MIBG SPECT/CT

SIOPEN score	Gold standard		P value
	Consistency	Inconsistency	
Planer imaging	151	87	<0.001
Tomography imaging	228	10	

^{123}I-MIBG, iodine-123-labeled metaiodobenzylguanidine; SPECT, single-photon emission computed tomography; CT, computed tomography; SIOPEN, International Society of Pediatric Oncology Europe Neuroblastoma.

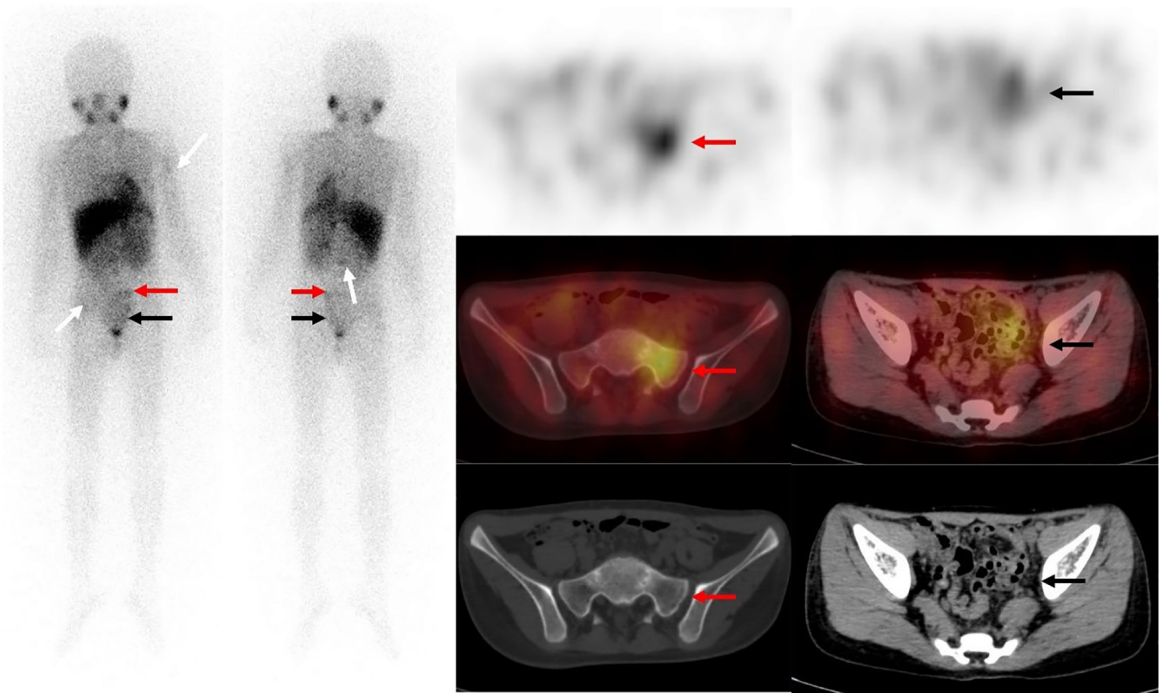

Figure 2 An 8-year-old boy had high-risk stage IV NB diagnosed by an outside institution. To assess the treatment efficacy, a ^{123}I-MIBG SPECT/CT was performed. The whole-body image (anterior and posterior) revealed multiple foci of intense activity (white arrows) but were not definite. However, on the axial images (SPECT, fusion, and CT), bone metastases were clearly visualized. There was an activity in pelvis, which had an intensity slightly higher than the background noise, which was easily determined to be intestinal activity. The SPECT/CT clearly showed that the upper activity (red arrows) represented sacral lesions, and the rest represented the physiological uptake by the colon (black arrows). NB, neuroblastoma; ^{123}I-MIBG, iodine-123-labeled metaiodobenzylguanidine; SPECT, single-photon emission computed tomography; CT, computed tomography.

Table 3 The difference between the different groups in ^{123}I-MIBG SPECT/CT

Planar imaging	Tomography imaging			Total	P value
	0	Low score	High score		
0	146	16	8	170	<0.001
Low score	12	18	9	39	
High score	0	2	27	29	
Total	158	36	44	238	

^{123}I-MIBG, iodine-123-labeled metaiodobenzylguanidine; SPECT, single-photon emission computed tomography; CT, computed tomography.

(*Table 6*). The sensitivity of diagnostic ability for metastases was 12.5%, the specificity was 94.7%, the PPV was 75%, the NPV was 46.2%, and the accuracy rate was 48.8%. We used the two methods to build a multifactor model via logistic regression with a cutoff value of 0.599 (95% CI, 0.483–0.823), a sensitivity of 40.9%, and a specificity of 88.9%.

Discussion

We found that ^{123}I-MIBG SPECT/CT was capable of altering the SIOPEN score to further improve the diagnostic ability of ^{123}I-MIBG and provide additional information about NB. However, our results did not examine the efficacy of PCR and FCM in detecting MRD

Table 4 The consistency of the SIOPEN score with the standard as compared across different imaging situations for the planar and tomographic images

Planar imaging	Gold standard						κ value
	0	1	2	3	4	≥5	
0	140	11	3	6	2	8	0.468
1	10	3	3	3	2	3	
2	2	0	2	1	1	1	
3	0	0	0	0	1	2	
4	0	0	0	1	1	3	
≥5	0	0	0	1	1	27	

SIOPEN, International Society of Pediatric Oncology Europe Neuroblastoma.

Table 5 The consistency of the SIOPEN score with the standard as compared across different imaging situations for the tomographic images

Tomography imaging	Gold standard						κ value
	0	1	2	3	4	≥5	
0	152	6	0	0	0	0	0.855
1	0	8	1	0	0	0	
2	0	0	7	1	0	0	
3	0	0	0	11	2	0	
4	0	0	0	0	6	0	
≥5	0	0	0	0	0	44	

SIOPEN, International Society of Pediatric Oncology Europe Neuroblastoma.

Table 6 The efficacy of MRD detection and ^{123}I-MIBG SPECT/CT

Parameters	P value	AUC	95% CI	Sensitivity	Specificity	PPV	NPV
PCR	0.024	0.649	0.485–0.810	0.400	0.895	0.833	0.531
FCM	0.416	0.540	0.362–0.710	0.125	0.947	0.750	0.462
SPECT/CT	0.000	–	–	0.928	0.944	0.897	0.962

MRD, minimal residual disease; ^{123}I-MIBG, iodine-123-labeled metaiodobenzylguanidine; SPECT, single-photon emission computed tomography; CT, computed tomography; AUC, area under the curve; CI, confidence interval; PPV, positive predictive value; NPV, negative predictive value; PCR, polymerase chain reaction (bone marrow); FCM, flow cytometry.

in the early detection of bone or bone marrow metastases.

Approximately 50% of patients with NB present with metastatic disease that typically involves bone and bone marrow, although soft tissue metastases may also occur (27). Thus, the accurate assessment of bone or bone marrow metastases and residual disease in children is clinically valuable for subsequent treatment selections, efficacy assessments, and prognosis prediction. Compared to conventional imaging, nuclear medicine imaging as a form of first-line functional imaging has high sensitivity (88–92%) and specificity (83–92%) (6). Matthay *et al.* (28) found that semiquantitative scoring in the early stage of treatment provides valuable prognostic information about overall survival and event-free survival, which enables children to achieve appropriate treatment outcomes. However, a number of interfering factors in clinical work affect planar

imaging, which results in an increase of false-negative and false-positive results (29).

To address these issues and improve the diagnostic accuracy, we performed ^{123}I-MIBG SPECT/CT, which is widely used in clinical practice (30). A total of 238 scans were included in this study, of which 81 (34%) had score changes (P<0.001). Gelfand *et al.* (31) showed that tomography did not increase the number of lesions but did improve the accuracy of image interpretation relative to planar imaging. Following advances in research, Fukuoka *et al.* reported (32) that ^{123}I-MIBG, SPECT/CT made 81% additional lesion findings compared to planar imaging, and the mean number of lesions was 3.0 *vs.* 3.7 for planar tomographic imaging, which is consistent with the results of our study.

In this study, the SIOPEN scores in the planar images changed from 0 to non-0 in 24 scans. Furthermore, the results were divided into the low-score group (a score of ≤4) and the high-score group (a score of >4) according to the SIOPEN cutoff score of 4. In total, 8 of the scans went from the 0-score group to the high-score group. A further analysis of the medical history and images showed that this might have occurred in some of the children because they had just received chemotherapy and were in the suppression period of chemotherapy; for other patients, this likely occurred because the degree of activity of the lesion was equal to or lower than the background noise, and in others because the ribs, thoracic spine, or sacrum had been missed due to the overlapping of the physiological uptake (e.g., by the liver or bladder), and the physiological uptake of the intestine was sometimes barely distinguishable from the pelvis metastases.

We examined the consistency of the two different imaging modalities in relation to the standard κ values and found that the consistency of planar imaging with the standard method was moderate (κ=0.468), while the consistency of the SPECT/CT imaging with the standard method was excellent (κ=0.855). Thus, the interreader agreement for SPECT/CT was considerably higher than that for planar images. In 4 of the scans, soft-tissue metastases were treated as bone metastases. In 5 other scans, due to the physiological uptake, muscle or renal pelvis filling, for example, was mistaken for metastases. In 3 other scans, issues occurred due to urine contamination. Thus, SPECT/CT imaging is clinically important in image interpretation, as depending on the results, such children may no longer receive subsequent treatments (33).

MRD is one of the main causes of recurrence in children with NB for early bone or bone marrow metastasis (34). MRD tests can detect the early infiltration of tumor cells in ≤5% of bone marrow, but sometimes clinical and imaging manifestations are not able to find bone metastases, thus, presently, MRD is a popular area of research (10). In this study, we analyzed the abilities of FCM and PCR, which are commonly used in the clinical detection of MRD, to detect bone marrow tumor cells. We found that FCM had low sensitivity. This may be because the ability of FCM to detect tumor cells is weakened due to the heterogeneity of the tumors and the treatment regimens. We also found that MRD detection with FCM is prone to false negatives, which may be because there is a lack of molecular markers with high specificity for NB cells. Seeger *et al.* (11) reported that 100 tumor cells per 105 nucleated bone marrow cells indicates a poor prognosis. Thus, the FCM technique has a good ability to detect MRD. The accuracy of the PCR method in detecting the *PHOX2B* gene in bone marrow is higher than that of the FCM method. We found that combining the FCM and PCR to detect the *PHOX2B* gene in the bone marrow improved the sensitivity (40.9%) of PCR and FCM methods, but the accuracy was not still as high as that of the ^{123}I-MIBG method (*Figure 3*). This limitation may be related to the detection site used to obtain tissues for the dynamic monitoring of tumor samples. However, as an invasive test, the MRD test causes some damage to children's bodies. During the clinical work, we found that some children who underwent the ^{123}I-MIBG test at our department tested negative for MRD, but lesions were detected in these children using ^{123}I-MIBG SPECT/CT (35).

This study had several limitations. First, the sample size was small, which limited our analysis, especially for MRD, and might have led to biased results. Second, the retrospective nature of the study might have caused selection bias. Additionally, Moss *et al.* (36) proposed that the immunocytologic analysis of bone marrow provides prognostic information; however, the children in the present study underwent a variety of treatments, including chemotherapy, radiotherapy, and immunotherapy, but only the value in assessing bone or bone marrow metastasis and recurrence was examined (37). Thus, further investigations need to be conducted to examine ^{123}I-MIBG SPECT/CT prognostic clinical role. Few international clinical studies have been conducted on the SIOPEN score. The MIBG metastasis assessment includes only whole-body bones without soft tissues, which is similar to the MRD test. Thus, the present research had some limitations in terms

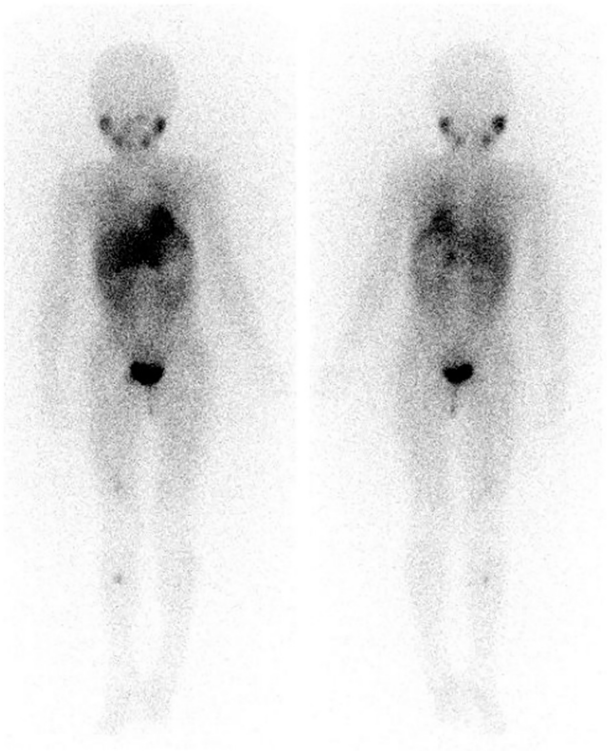

Figure 3 A 5-year-old girl was pathologically confirmed to have high-risk stage IV NB. She had received surgery, chemotherapy, and radiotherapy 2 years prior. A routine surveillance ^{123}I-MIBG SPECT/CT was performed. The whole-body images (anterior and posterior) reveled osseous metastasis. However, the MRD results of the previous day were negative. Both FCM assays and PCR were used to detect the bone marrow tumor cells. NB, neuroblastoma; ^{123}I-MIBG, iodine-123-labeled metaiodobenzylguanidine; SPECT, single-photon emission computed tomography; CT, computed tomography; MRD, minimal residual disease; FCM, flow cytometry; PCR, polymerase chain reaction (bone marrow).

of monitoring high-risk recurrence and prognosis. We intend to expand the sample size of the study and conduct a prospective study in the future.

Conclusions

In summary, we found that ^{123}I-MIBG SPECT/CT increased the diagnostic ability to discover more lesions and the accuracy of the lesions, could be used to obtain a precise SIOPEN score, and thus could be used to design improved treatment strategies and prevent unnecessary work. The diagnostic performance of the MRD test was inferior to that of the ^{123}I-MIBG SPECT/CT; however, MRD can also be used to discover early metastasis and recurrence in the bone or bone marrow, and its prognostic value needs to be further investigated.

Acknowledgments

The authors would like to thank the staff members at Beijing Friendship Hospital, Affiliated to Capital Medical University and Department of Nuclear Medicine, for their assistance in carrying out this study.
Funding: This work was supported by the National Natural Science Foundation of China (Nos. 82102088, 82272034, 82001860, 81971642, and 82001861), Capital's Funds for Health Improvement and Research (No. 2020-2-2025), and the National Key Research and Development Plan (No. 2020YFC0122000).

Footnote

Reporting Checklist: The authors have completed the STARD reporting checklist. Available at https://qims.amegroups.com/article/view/10.21037/qims-22-1120/rc

Conflicts of Interest: All authors have completed the ICMJE uniform disclosure form (available at https://qims.amegroups.com/article/view/10.21037/qims-22-1120/coif). The authors have no conflicts of interest to declare.

Ethical Statement: The authors are accountable for all aspects of the work, including ensuring that any questions related to the accuracy or integrity of any part of the work have been appropriately investigated and resolved. The study was conducted in accordance with the Declaration of Helsinki (as revised in 2013). The study was approved by the Institutional Board of the Beijing Friendship Hospital of Capital Medical University (No. 2022-P3-324-01), and the requirement of individual consent for this retrospective analysis was waived.

References

1. Ward E, DeSantis C, Robbins A, Kohler B, Jemal A. Childhood and adolescent cancer statistics, 2014. CA Cancer J Clin 2014;64:83-103.
2. Matthay KK, Maris JM, Schleiermacher G, Nakagawara A, Mackall CL, Diller L, Weiss WA. Neuroblastoma. Nat Rev Dis Primers 2016;2:16078.
3. Swift CC, Eklund MJ, Kraveka JM, Alazraki AL. Updates in Diagnosis, Management, and Treatment of Neuroblastoma. Radiographics 2018;38:566-80.
4. Whittle SB, Smith V, Doherty E, Zhao S, McCarty S, Zage PE. Overview and recent advances in the treatment of neuroblastoma. Expert Rev Anticancer Ther 2017;17:369-86.
5. Kushner BH. Neuroblastoma: a disease requiring a multitude of imaging studies. J Nucl Med 2004;45:1172-88.
6. Sharp SE, Trout AT, Weiss BD, Gelfand MJ. MIBG in Neuroblastoma Diagnostic Imaging and Therapy. Radiographics 2016;36:258-78.
7. Sharp SE, Parisi MT, Gelfand MJ, Yanik GA, Shulkin BL. Functional-metabolic imaging of neuroblastoma. Q J Nucl Med Mol Imaging 2013;57:6-20.
8. Olecki E, Grant CN. MIBG in neuroblastoma diagnosis and treatment. Semin Pediatr Surg 2019;28:150859.
9. Decarolis B, Schneider C, Hero B, Simon T, Volland R, Roels F, Dietlein M, Berthold F, Schmidt M. Iodine-123 metaiodobenzylguanidine scintigraphy scoring allows prediction of outcome in patients with stage 4 neuroblastoma: results of the Cologne interscore comparison study. J Clin Oncol 2013;31:944-51.
10. Park JR, Bagatell R, Cohn SL, Pearson AD, Villablanca JG, Berthold F, Burchill S, Boubaker A, McHugh K, Nuchtern JG, London WB, Seibel NL, Lindwasser OW, Maris JM, Brock P, Schleiermacher G, Ladenstein R, Matthay KK, Valteau-Couanet D. Revisions to the International Neuroblastoma Response Criteria: A Consensus Statement From the National Cancer Institute Clinical Trials Planning Meeting. J Clin Oncol 2017;35:2580-7.
11. Seeger RC, Reynolds CP, Gallego R, Stram DO, Gerbing RB, Matthay KK. Quantitative tumor cell content of bone marrow and blood as a predictor of outcome in stage IV neuroblastoma: a Children's Cancer Group Study. J Clin Oncol 2000;18:4067-76.
12. Cheung NK, Ostrovnaya I, Kuk D, Cheung IY. Bone marrow minimal residual disease was an early response marker and a consistent independent predictor of survival after anti-GD2 immunotherapy. J Clin Oncol 2015;33:755-63.
13. Uemura S, Ishida T, Thwin KKM, Yamamoto N, Tamura A, Kishimoto K, Hasegawa D, Kosaka Y, Nino N, Lin KS, Takafuji S, Mori T, Iijima K, Nishimura N. Dynamics of Minimal Residual Disease in Neuroblastoma Patients. Front Oncol 2019;9:455.
14. Schriegel F, Taschner-Mandl S, Bernkopf M, Grunwald U, Siebert N, Ambros PF, Ambros I, Lode HN, Henze G, Ehlert K. Comparison of three different methods to detect bone marrow involvement in patients with neuroblastoma. J Cancer Res Clin Oncol 2022;148:2581-8.
15. Stutterheim J, Gerritsen A, Zappeij-Kannegieter L, Kleijn I, Dee R, Hooft L, van Noesel MM, Bierings M, Berthold F, Versteeg R, Caron HN, van der Schoot CE, Tytgat GA. PHOX2B is a novel and specific marker for minimal residual disease testing in neuroblastoma. J Clin Oncol 2008;26:5443-9.
16. Ben Lassoued A, Nivaggioni V, Gabert J. Minimal residual disease testing in hematologic malignancies and solid cancer. Expert Rev Mol Diagn 2014;14:699-712.
17. Liu B, Servaes S, Zhuang H. SPECT/CT MIBG Imaging Is Crucial in the Follow-up of the Patients With High-Risk Neuroblastoma. Clin Nucl Med 2018;43:232-8.
18. Pott C, Sehn LH, Belada D, Gribben J, Hoster E, Kahl B, Kehden B, Nicolas-Virelizier E, Spielewoy N, Fingerle-Rowson G, Harbron C, Mundt K, Wassner-Fritsch E, Cheson BD. MRD response in relapsed/refractory FL after obinutuzumab plus bendamustine or bendamustine alone in the GADOLIN trial. Leukemia 2020;34:522-32.
19. Olivier P, Colarinha P, Fettich J, Fischer S, Frökier J, Giammarile F, Gordon I, Hahn K, Kabasakal L, Mann M, Mitjavila M, Piepsz A, Porn U, Sixt R, van Velzen J. Guidelines for radioiodinated MIBG scintigraphy in children. Eur J Nucl Med Mol Imaging 2003;30:B45-50.
20. Bar-Sever Z, Biassoni L, Shulkin B, Kong G, Hofman MS, Lopci E, Manea I, Koziorowski J, Castellani R, Boubaker A, Lambert B, Pfluger T, Nadel H, Sharp S, Giammarile F. Guidelines on nuclear medicine imaging in neuroblastoma. Eur J Nucl Med Mol Imaging 2018;45:2009-24.
21. Bombardieri E, Giammarile F, Aktolun C, Baum RP, Bischof Delaloye A, Maffioli L, Moncayo R, Mortelmans L, Pepe G, Reske SN, Castellani MR, Chiti A; European Association for Nuclear Medicine. 131I/123I-metaiodobenzylguanidine (mIBG) scintigraphy: procedure guidelines for tumour imaging. Eur J Nucl Med Mol Imaging 2010;37:2436-46.

22. Beiske K, Ambros PF, Burchill SA, Cheung IY, Swerts K. Detecting minimal residual disease in neuroblastoma patients-the present state of the art. Cancer Lett 2005;228:229-40.
23. Zirngibl F, Ivasko SM, Grunewald L, Klaus A, Schwiebert S, Ruf P, Lindhofer H, Astrahantseff K, Andersch L, Schulte JH, Lode HN, Eggert A, Anders K, Hundsdoerfer P, Künkele A. GD2-directed bispecific trifunctional antibody outperforms dinutuximab beta in a murine model for aggressive metastasized neuroblastoma. J Immunother Cancer 2021;9:e002923.
24. Matthay KK, Shulkin B, Ladenstein R, Michon J, Giammarile F, Lewington V, Pearson AD, Cohn SL. Criteria for evaluation of disease extent by (123) I-metaiodobenzylguanidine scans in neuroblastoma: a report for the International Neuroblastoma Risk Group (INRG) Task Force. Br J Cancer 2010;102:1319-26.
25. Lewington V, Lambert B, Poetschger U, Sever ZB, Giammarile F, McEwan AJB, Castellani R, Lynch T, Shulkin B, Drobics M, Staudenherz A, Ladenstein R. (123) I-mIBG scintigraphy in neuroblastoma: development of a SIOPEN semi-quantitative reporting ,method by an international panel. Eur J Nucl Med Mol Imaging 2017;44:234-41.
26. Landis JR, Koch GG. The measurement of observer agreement for categorical data. Biometrics 1977;33:159-74.
27. Polishchuk AL, Li R, Hill-Kayser C, Little A, Hawkins RA, Hamilton J, Lau M, Tran HC, Strahlendorf C, Lemons RS, Weinberg V, Matthay KK, DuBois SG, Marcus KJ, Bagatell R, Haas-Kogan DA. Likelihood of bone recurrence in prior sites of metastasis in patients with high-risk neuroblastoma. Int J Radiat Oncol Biol Phys 2014;89:839-45.
28. Matthay KK, Edeline V, Lumbroso J, Tanguy ML, Asselain B, Zucker JM, Valteau-Couanet D, Hartmann O, Michon J. Correlation of early metastatic response by 123I-metaiodobenzylguanidine scintigraphy with overall response and event-free survival in stage IV neuroblastoma. J Clin Oncol 2003;21:2486-91.
29. Satharasinghe K, Trahair TN, Barbaric D, O'Brien TA, Russell SJ, Cohn RJ, Marshall GM, Ziegler DS. False-positive MIBG scans with normal computed tomography imaging in patients with high-risk neuroblastoma. J Clin Oncol 2009;27:e233-4; author reply e235.
30. Roach PJ, Schembri GP, Ho Shon IA, Bailey EA, Bailey DL. SPECT/CT imaging using a spiral CT scanner for anatomical localization: Impact on diagnostic accuracy and reporter confidence in clinical practice. Nucl Med Commun 2006;27:977-87.
31. Gelfand MJ, Elgazzar AH, Kriss VM, Masters PR, Golsch GJ. Iodine-123-MIBG SPECT versus planar imaging in children with neural crest tumors. J Nucl Med 1994;35:1753-7.
32. Fukuoka M, Taki J, Mochizuki T, Kinuya S. Comparison of diagnostic value of I-123 MIBG and high-dose I-131 MIBG scintigraphy including incremental value of SPECT/CT over planar image in patients with malignant pheochromocytoma/paraganglioma and neuroblastoma. Clin Nucl Med 2011;36:1-7.
33. Messina JA, Cheng SC, Franc BL, Charron M, Shulkin B, To B, Maris JM, Yanik G, Hawkins RA, Matthay KK. Evaluation of semi-quantitative scoring system for metaiodobenzylguanidine (mIBG) scans in patients with relapsed neuroblastoma. Pediatr Blood Cancer 2006;47:865-74.
34. Luskin MR, Murakami MA, Manalis SR, Weinstock DM. Targeting minimal residual disease: a path to cure? Nat Rev Cancer 2018;18:255-63.
35. Hillengass J, Merz M, Delorme S. Minimal residual disease in multiple myeloma: use of magnetic resonance imaging. Semin Hematol 2018;55:19-21.
36. Moss TJ, Reynolds CP, Sather HN, Romansky SG, Hammond GD, Seeger RC. Prognostic value of immunocytologic detection of bone marrow metastases in neuroblastoma. N Engl J Med 1991;324:219-26.
37. Burchill SA, Beiske K, Shimada H, Ambros PF, Seeger R, Tytgat GA, Brock PR, Haber M, Park JR, Berthold F. Recommendations for the standardization of bone marrow disease assessment and reporting in children with neuroblastoma on behalf of the International Neuroblastoma Response Criteria Bone Marrow Working Group. Cancer 2017;123:1095-105.

Cite this article as: Zhou Z, Wang G, Qian L, Liu J, Yang X, Zhang S, Zhang M, Kan Y, Wang W, Yang J. Evaluation of iodine-123-labeled metaiodobenzylguanidine single-photon emission computed tomography/computed tomography based on the International Society of Pediatric Oncology Europe Neuroblastoma score in children with neuroblastoma. Quant Imaging Med Surg 2023;13(6):3841-3851. doi: 10.21037/qims-22-1120

